



PRISM: Pushing the Frontier of Deep Think via Process Reward Model-Guided Inference

Rituraj Sharma^{*}  Weiyuan Chen^{*}  Noah Provenzano  Tu Vu 
 Virginia Tech

{rituraj, cweiyuan9, noahpro, tuvuv}@vt.edu

 <https://github.com/Rituraj003/PRISM/>

Abstract

DEEPTHINK methods improve reasoning by generating, refining, and aggregating populations of candidate solutions, which enables strong performance on complex mathematical and scientific tasks. However, existing frameworks often lack reliable correctness signals during inference, which creates a population-enhancement bottleneck where deeper deliberation amplifies errors, suppresses correct minority solutions, and yields weak returns to additional compute. In this paper, we introduce a functional decomposition of DEEPTHINK systems and propose PRISM, a Process Reward Model (PRM)-guided inference algorithm that uses step-level verification to guide both population refinement and solution aggregation. During refinement, PRISM treats candidate solutions as particles in a PRM-defined energy landscape and reshapes the population through score-guided resampling and stochastic refinement, which concentrates probability mass on higher-quality reasoning while preserving diversity. Across mathematics and science benchmarks, PRISM is competitive with or outperforms existing DEEPTHINK methods, reaching 90.0%, 75.4%, and 71.4% with gpt-oss-20b on AIME25, HMMT25, and GPQA Diamond, respectively, while matching or exceeding gpt-oss-120b. Additionally, our analysis shows that PRISM produces consistent net-directional correction during refinement, remains reliable when the initial population contains few correct candidates, and often lies on the compute-accuracy Pareto frontier.

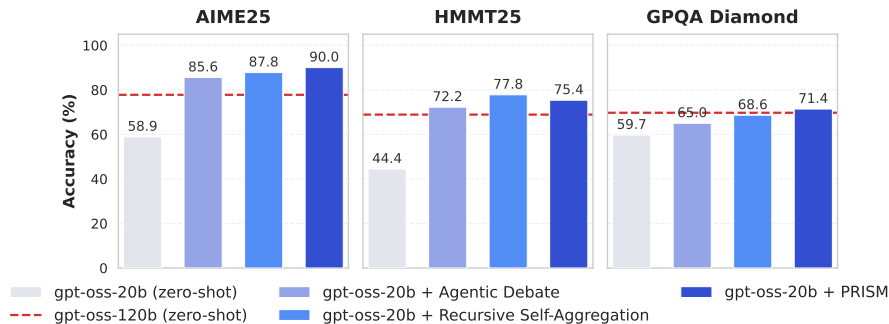


Figure 1: **Accuracy on AIME25, HMMT25, and GPQA Diamond.** PRISM achieves competitive or superior performance relative to state-of-the-art DEEPTHINK methods, enabling gpt-oss-20b to match or exceed gpt-oss-120b (see Table 1 for more results).

^{*}Co-first authors.

1 Introduction

Recent advances in large language models (LLMs) have led to the emergence of DEEP THINK, a reasoning paradigm that allocates additional inference-time compute to simultaneously explore and combine multiple candidate solutions before producing a final answer [Google, 2025, 2026]. DEEP THINK systems have demonstrated state-of-the-art performance on rigorous reasoning benchmarks and have reached gold-medal standards in competitions such as the International Mathematical Olympiad [Luong and Lockhart, 2025] and the International Collegiate Programming Contest [Lin and Cheng, 2025]. Furthermore, these systems are increasingly used as research collaborators in mathematical and scientific discovery, where they support knowledge retrieval and rigorous verification [Luong and Mirrokni, 2026].

Despite their successes, DEEP THINK systems remain poorly understood at a mechanistic level. Most existing frameworks are presented as monolithic pipelines, which makes it difficult to attribute improvements to specific design choices, diagnose failure modes, or understand the compute-performance tradeoff. Such a framing also obscures how components interact during extended reasoning, which limits systematic improvement and principled comparison across methods. This lack of transparency is concerning, since increased reasoning capability does not automatically translate into improved safety [Phan et al., 2025].

To address this gap, we introduce a functional taxonomy of DEEP THINK frameworks that decomposes existing methods into three stages: *population creation*, which generates diverse candidate solutions; *population enhancement* (also referred to as *population refinement*), which iteratively refines and improves these candidates; and *solution aggregation*, which selects the final answer (see Figure 2, *top*). This decomposition enables systematic analysis and controlled comparison across methods.

Through this lens, we identify population enhancement as the primary bottleneck for improving both accuracy and efficiency. Across evaluation benchmarks, we observe that simple parallel sampling followed by majority voting performs competitively with several sophisticated DEEP THINK systems, which indicates that much of the observed performance arises from initial population diversity and aggregation rather than iterative refinement.

Our taxonomy further reveals key limitations of current refinement strategies. Many repeatedly rewrite or rework entire solutions without a stable quality signal. As a result, increasing refinement depth (the number of refinement iterations) does not reliably improve population quality, and errors may persist, propagate, or amplify across iterations. Approaches that rely on majority-based enhancement, which steers candidates toward the most frequent solution, provide partial guidance through consensus but introduce a complementary failure mode: infrequent yet logically correct reasoning traces are suppressed by more frequent but incorrect trajectories, a phenomenon we refer to as *majority dilution*. Consequently, current systems often fail to fully exploit their generated populations and exhibit suboptimal compute-performance tradeoffs.

Motivated by these findings, we propose PRISM (**P**rocess reward model-guided **R**efinement, **I**teration, and **S**election **M**echanisms), an inference algorithm that introduces explicit step-level correctness signals into both population refinement and solution aggregation (Figure 2, *bottom*). PRISM uses a Process Reward Model (PRM) to evaluate reasoning trajectories based on their internal steps, which provides quality feedback independent of how frequently a trajectory appears in the population. During refinement, PRISM treats candidate solutions as particles in an energy landscape defined by PRM scores and iteratively concentrates probability mass on higher-quality reasoning through score-guided resampling and stochastic mutation. These Markov chain Monte Carlo (MCMC)-style transitions balance exploitation of promising solutions with continued exploration, transforming refinement from stochastic rewriting into directional error correction. The final prediction is obtained by selecting the candidate with the highest aggregate PRM score across reasoning steps.

Across mathematical and scientific reasoning benchmarks, PRISM is competitive with or outperforms state-of-the-art DEEP THINK methods, achieving 90.0%, 75.4%, and 71.4% with `gpt-oss-20b` on AIME25, HMMT25, and GPQA Diamond, respectively, while matching or exceeding `gpt-oss-120b` [Agarwal et al., 2025]. Beyond accuracy, our analysis shows that PRISM mitigates key failure modes of prior DEEP THINK methods. In particular, PRISM produces net-directional corrections during refinement, exhibiting a strongly positive *NetFlip*, which indicates that incorrect solutions are corrected more often than correct ones are degraded. In low-correctness regimes, where the initial population contains few valid solutions, PRISM avoids suppressing correct minority traces and instead

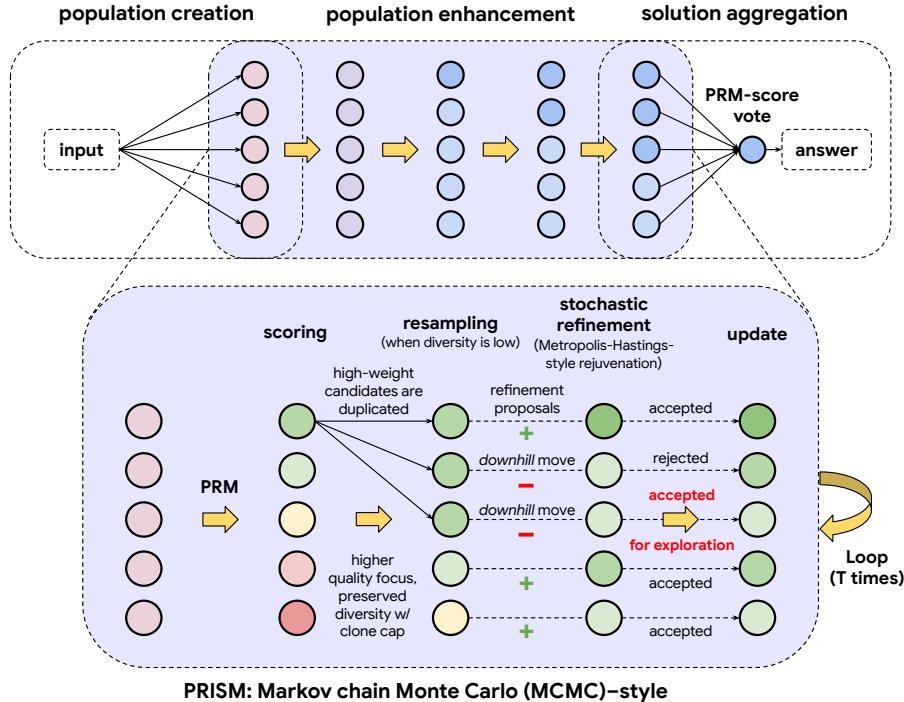


Figure 2: **Functional taxonomy of DEEPTHINK systems (top) and overview of PRISM (bottom).** The top panel decomposes DEEPTHINK into *population creation*, *population enhancement*, and *solution aggregation*. The bottom panel illustrates PRISM’s refinement mechanism, which uses Process Reward Model (PRM)-defined scores to guide resampling and stochastic refinement within an energy-based population framework.

bootstraps from weak populations by filtering harmful updates and amplifying promising partial reasoning. Finally, PRISM often lies on or near the compute–accuracy Pareto frontier under fixed budgets, which shows that additional inference-time compute translates efficiently into improved correctness.

To summarize, our main contributions are:

- **A functional taxonomy of DEEPTHINK systems:** We decompose existing frameworks into population creation, enhancement, and aggregation, which sheds light on their internal mechanisms and identifies population enhancement as the primary bottleneck for improving accuracy and compute efficiency.
- **New method:** We propose PRISM, a PRM-guided inference algorithm that uses step-level correctness signals to transform iterative refinement into directional error correction and inform final solution aggregation.
- **Improved performance, robustness, and scaling behavior:** We show that across rigorous academic benchmarks, PRISM is competitive with or outperforms state-of-the-art DEEPTHINK methods, produces consistent net-directional correction during refinement, remains reliable in low-correctness regimes, and often lies on the compute-accuracy Pareto frontier.

Taken as a whole, we hope that our work will spur more principled research into scalable and reliable inference-time reasoning.

2 Dissecting DEEPTHINK frameworks

In this section, we introduce a functional decomposition of DEEPTHINK frameworks into population creation, enhancement, and aggregation. Through this lens, we identify a population-refinement bottleneck and present empirical observations that motivate our method introduced in Section 3.

2.1 A functional taxonomy of DEEP THINK frameworks

We decompose DEEP THINK frameworks into three stages: *population creation* (generating candidate solutions), *population enhancement* (iteratively refining candidates), and *solution aggregation* (synthesizing the answer). Each framework can be understood as instantiating these stages through distinct design choices. This decomposition isolates the role of each stage in shaping reasoning quality and enables a mechanistic analysis of how additional compute translates into correctness.

Population creation: This stage generates an initial, diverse set of candidate reasoning trajectories. The most common approach produces multiple candidates independently via stochastic decoding (e.g., temperature or nucleus sampling [Holtzman et al., 2020]), as in Wang et al. [2023]; we refer to this strategy as **Sample-N**. An alternative is single-pass multi-candidate generation, where the model produces several solutions within one generation, sometimes with associated plausibility signals (e.g., verbalized sampling [Zhang et al., 2025]). Population creation primarily contributes diversity rather than correctness: it increases the probability that at least one correct trajectory exists but does not concentrate probability mass on correct solutions. Consequently, downstream performance depends critically on how effectively later stages identify and amplify high-quality candidates.

Population enhancement: This stage operates on the initially generated candidate population and iteratively refines candidates with the goal of increasing the density of correct reasoning trajectories while preserving useful diversity [Choi et al., 2025]. Existing methods fall into several broad categories, including *critic-guided refinement*, which uses a critic to verify and revise each candidate solution independently [Chai et al., 2025]; *multi-agent interaction*, where agents iteratively challenge and update one another’s reasoning [Wang et al., 2025]; *consensus-driven updating*, which steers candidates toward the majority belief in the population [Choi et al., 2025]; and *aggregation-based refinement*, which recursively recombines candidate solutions to produce improved ones [Venkatraman et al., 2025]. Despite differing mechanisms, these methods share a common objective: to improve population quality across refinement depth.

In practice, however, population enhancement is often the least reliable stage. Refinement can propagate early errors, suppress correct minority trajectories, or drift toward frequent but incorrect reasoning patterns. As a result, population quality often oscillates or degrades rather than improving monotonically with additional refinement, which creates a population-enhancement bottleneck.

Solution aggregation: This stage converts the final candidate population into a single prediction. The most common mechanism selects the most frequent answer among candidates (Majority Vote). More expressive strategies use model-based aggregation, where an LLM synthesizes a final answer by conditioning on the entire population (LLM Aggregate). However, aggregation implicitly assumes that population enhancement has produced a sufficiently high-quality candidate set. When this assumption fails, aggregation can amplify noise rather than correct it, which further highlights the role of population enhancement in determining overall performance. In this work, we additionally explore PRM-guided correctness-aware aggregation (PRM-score Vote), which selects the candidate with the highest aggregate PRM score.

2.2 Empirical motivation: The population-refinement bottleneck

DEEP THINK frameworks implicitly rely on a *monotonic refinement assumption*: additional refinement iterations should progressively improve population quality and translate into higher final accuracy. Under controlled conditions where population creation is *fixed* and only enhancement and aggregation vary, we find that this assumption frequently breaks down.

First, *diversity combined with simple aggregation is already a strong baseline*. Parallel sampling followed by majority voting often achieves competitive performance at low compute, while several refinement-heavy frameworks yield only marginal gains despite substantially higher token usage. Second, *increasing refinement depth does not reliably improve population quality*. Across settings, the fraction of correct candidates often oscillates and can degrade over successive refinement iterations, which indicates that refinement updates often behave as stochastic perturbations rather than directional improvements. Finally, *aggregation performance depends critically on the output of population enhancement*. When the candidate population is noisy, aggregation mechanisms can reinforce or rationalize incorrect majorities instead of filtering them (see Section 5.2 for details).

Taken as a whole, these findings reveal a *population-refinement bottleneck*. Without a correctness-sensitive signal, refinement updates can preserve, propagate, or amplify errors, which limits the

Algorithm 1 PRM-guided Resampling and Informed Stochastic Mutation.

Input: Initial population $\mathcal{P}^{(0)} = \{\tau_i^{(0)}\}_{i=1}^N$, verifier V (PRM), iterator I , comparator C

Hyperparameters: depth T , T_{smc} , ESS threshold α , noise η , clamp c , clone cap κ

Output: Updated population $\mathcal{P}^{(T)}$

```
1: for  $t = 1$  to  $T$  do
  SCORING
2:   for all  $\tau_i \in \mathcal{P}^{(t-1)}$  in parallel do
3:      $\tau_i \leftarrow \text{STEPWISENORMALIZE}(\tau_i)$ 
4:      $\text{fb}_i \leftarrow V(\tau_i)$ ;  $s_i \leftarrow \text{SCORE}(\text{fb}_i) \in [0, 1]$ 
5:      $w_i \leftarrow s_i^{1/T_{\text{smc}}}$ 
6:   end for
7:    $(\mathcal{P}^{(t-1)}, \{s_i\}) \leftarrow \text{ARBITRATE}(\mathcal{P}^{(t-1)}, \{s_i, \text{fb}_i\}, C, c)$ 
8:    $w_i \leftarrow s_i^{1/T_{\text{smc}}}$ 
  RESAMPLING
9:    $\text{ESS} \leftarrow \frac{(\sum_i w_i)^2}{\sum_i w_i^2}$ 
10:  if  $\text{ESS} < \alpha N$  then
11:     $\mathcal{P}^{(t-1)} \leftarrow \text{SYSTEMATICRESAMPLE}(\mathcal{P}^{(t-1)}, \{w_i\})$ 
12:     $\mathcal{P}^{(t-1)} \leftarrow \text{CAPCOPIES}(\mathcal{P}^{(t-1)}, \lceil \kappa N \rceil)$ 
13:  end if
  STOCHASTIC REFINEMENT (Metropolis-Hastings-style rejuvenation)
14:  for all  $\tau_i \in \mathcal{P}^{(t-1)}$  in parallel do
15:     $\tau'_i \leftarrow I(\tau_i, \text{fb}_i; \eta)$   $\triangleright$  inject “different approach” w.p.  $\eta$ 
16:     $\text{fb}'_i \leftarrow V(\tau'_i)$ ;  $s'_i \leftarrow \text{SCORE}(\text{fb}'_i)$ 
17:    accept  $\tau'_i$  w.p.  $\min(1, (s'_i/s_i)^{1/T_{\text{smc}}})$ 
18:  end for
19:   $\mathcal{P}^{(t)} \leftarrow \text{UPDATEPARTICLES}(\mathcal{P}^{(t-1)}, \{\tau'_i\})$ 
20: end for
21: return  $\mathcal{P}^{(T)}$ 
```

returns from additional inference-time compute and prevents systems from fully exploiting their candidate populations. Overcoming this bottleneck requires inference mechanisms that incorporate explicit correctness signals to guide both population refinement and aggregation.

3 PRISM: PRM-guided Refinement, Iteration, and Selection Mechanisms

We propose PRISM, a Process Reward Model (PRM)-guided inference algorithm that addresses the population-refinement bottleneck by injecting explicit step-level correctness signals into both refinement dynamics and final selection.

During refinement, PRISM treats candidate reasoning traces as a population evolving under an energy landscape defined by the PRM, where higher-quality reasoning corresponds to lower energy. Intuitively, refinement progressively reallocates probability mass toward lower-energy regions while preserving controlled exploration. Each refinement iteration performs *three* operations: **scoring**, **resampling**, and **stochastic refinement**. First, PRISM evaluates every candidate using PRM step-level feedback and converts scores into temperature-controlled importance weights. Second, it monitors population diversity and resamples when probability mass collapses onto a small subset of candidates (diversity is low). Third, it proposes stochastic refinements that are accepted probabilistically based on PRM scores, which enables directional error correction while avoiding deterministic overwriting. Algorithm 1 summarizes the procedure.

Scoring: Let V denote the PRM and τ a candidate reasoning trace sampled from the generator G . Before scoring, we deterministically coerce τ into an explicit stepwise representation,¹ i.e., $\tau \leftarrow \text{STEPWISENORMALIZE}(\tau)$. The PRM then generates step-level feedback $\text{fb} = V(\tau)$, which we

¹The normalizer first parses existing `<step>` blocks and, if none are found, splits on blank lines and wraps each segment in `<step>` tags.

map to a scalar consistency score $s(\tau) \in [0, 1]$ using a deterministic rule $\text{SCORE}(\cdot)$ (See Appendix A.3 for details), where higher values indicate stronger internal coherence. We then convert this score into an unnormalized importance weight

$$w(\tau) \propto s(\tau)^{1/T_{\text{smc}}}, \quad (1)$$

where T_{smc} controls the exploration-exploitation tradeoff (smc stands for Sequential Monte Carlo). Lower temperatures concentrate probability mass on high-scoring candidates, while higher temperatures preserve diversity. This weighting defines an implicit energy landscape over reasoning trajectories and corresponds to a Boltzmann (Gibbs) distribution with energy $E(\tau) = -\log(s_\tau)$.

Population management via resampling: Importance weighting can concentrate probability mass on a small subset of candidates, which we quantify by computing the *effective sample size (ESS)*

$$\text{ESS} = \frac{(\sum_i w_i)^2}{\sum_i w_i^2}. \quad (2)$$

If ESS falls below a threshold (e.g., αN),² we resample: high-weight candidates are duplicated and low-weight candidates discarded. Resampling reallocates compute toward promising trajectories while maintaining population-level stability.

Stochastic refinement (Metropolis-Hastings-style rejuvenation): Resampling redistributes probability mass but does not introduce new reasoning directions. To enable correction and exploration, PRISM applies a stochastic refinement move to each candidate.

Given a current trace τ , an iterator model I proposes a refined trace using PRM feedback. Most proposals perform local refinements to the current reasoning, while a small fraction (which is controlled by a hyperparameter η) introduce alternative reasoning directions to maintain exploration (See Appendix B.1). Define the acceptance ratio

$$r_w = \frac{w(\tau')}{w(\tau)} = \left(\frac{s(\tau')}{s(\tau)} \right)^{1/T_{\text{smc}}}, \quad (3)$$

The proposal is accepted with probability $A(\tau \rightarrow \tau') = \min(1, r_w)$, which favors increases in PRM score while still occasionally accepting score-decreasing moves, helping the refinement process escape local modes. This turns refinement into a score-guided local search rather than independent rewriting.³

Practical safeguards: We incorporate two stabilizers to prevent pathological population dynamics: (i) **conflict arbitration** resolves cases where distinct answers receive similarly high PRM scores by using a comparator model and clamping conflicting candidates to a minimum score c (See Appendix C.1; and (ii) **clone capping** limits the fraction k of the population that can be occupied by duplicated traces during resampling, which prevents pathological collapse and keeps behavior invariant to population size.

PRM-guided solution aggregation: After refinement, PRISM converts the final candidate population $P^{(T)} = \{\tau_i\}_{i=1}^N$ into a single prediction using PRM-score voting. For each unique extracted answer a , we aggregate its PRM score

$$S(a) = \sum_{i: \text{Ans}(\tau_i)=a} s(\tau_i), \quad (4)$$

where $\text{Ans}(\tau_i)$ denotes the answer extracted from trajectory τ_i . The final prediction is then $\hat{a} = \arg \max_a S(a)$. This aggregation favors answers supported by higher-quality reasoning rather than by frequency alone.

²ESS ranges from 1 to the population size N . A high ESS indicates relatively uniform weights and preserved diversity, while a low ESS indicates collapse, where a small number of trajectories dominate the population.

³Because the proposal operator I is an LLM with intractable proposal density, we use a Metropolis-inspired energy-based acceptance filter (via weight ratios) rather than claiming an exact Metropolis–Hastings correction.

4 Experimental setup

Having established our PRISM method, we now evaluate its effectiveness as an end-to-end inference algorithm. Our goal is to measure how different DEEPTHINK methods translate additional compute into accuracy. To enable a controlled comparison, all methods share the same inference configuration, including identical backbone models, population width, refinement depth, and initialization. Token usage may vary across methods and is reported explicitly. We fix population creation using Sample-N so that all methods operate on the same initial candidates. For solution aggregation, we report majority voting and LLM-based aggregation for all methods, while PRISM additionally supports PRM-score voting as part of its inference procedure. Below, we describe the baselines, benchmarks, models, inference protocol, and evaluation metrics.

4.1 Baselines

We compare PRISM with a diverse set of representative methods that differ in how they allocate compute across candidate solutions.

Simple Voting (no refinement): The final answer is selected by majority vote or PRM-score vote over the initial candidate population without iterative refinement.

SciMaster [Chai et al., 2025]: Each candidate reasoning trace is independently critiqued and rewritten at every iteration. This method focuses on local error correction but rewrites entire solutions without an explicit correctness signal.

Agentic Debate [Wang et al., 2025]: A multi-agent framework in which each candidate revises itself using information from other candidates in the population, enabling peer-to-peer information flow. This collaborative refinement can improve consensus but may reinforce shared errors.

MAD Conformist [Choi et al., 2025]: A majority-driven framework that anchors the population to the current majority answer. Candidates that agree with the majority are preserved, while non-conforming candidates are selectively refined toward consensus.

MAD Follower [Choi et al., 2025]: A majority-driven variant that replaces a fraction of the population with candidates that explicitly adopt the majority solution before refinement. This more aggressively steers the population toward agreement.

Recursive Self-Aggregation [Venkatraman et al., 2025]: An aggregation-driven framework that repeatedly synthesizes subsets of candidate solutions into new aggregate solutions, which are then reintroduced into the population.

4.2 Evaluation benchmarks

We evaluate on three reasoning benchmarks: AIME25 and HMMT25 from MathArena [Balunovic et al., 2025], and GPQA Diamond [Rein et al., 2024]. Since DEEPTHINK inference is compute-intensive, we cap GPQA Diamond at the first 120 examples to keep evaluation tractable. AIME25 and HMMT25 are evaluated in full.

4.3 Models

We evaluate nine generator models across two families. We use `gpt-oss-20b` as the primary backbone for PRISM and other DEEPTHINK methods, while `gpt-oss-120b` serves mainly as a strong zero-shot baseline. We also experiment with the Qwen3 family [Yang et al., 2025], including Qwen-1.7B, Qwen-4B, Qwen-14B, and Qwen-30B-A3B (hybrid pretrained + post-trained variants). We further evaluate three additional Qwen-4B variants (Base, Instruct, and Thinking) to examine how PRISM interacts with models that differ in training objective and reasoning specialization.

Unless otherwise specified, the generator G , verifier V , iterator I , and comparator C models are all instantiated from the same backbone model (Appendices A, B, C contain the prompts). One exception is our cross generator-verifier scaling experiment (Section 5.3), where the verifier is allowed to differ in size from the generator to study the effect of verifier strength. For the generator and iterator, which require diverse responses for DEEPTHINK, we use stochastic decoding with temperature = 0.8 and $top_p = 0.9$. For the verifier and comparator, we always use deterministic decoding (temperature = 0).

4.4 Inference protocol

For each problem, we sample from the generator to initialize a population of $N = 10$ candidate reasoning traces. These traces form the shared starting point for all methods. Each method then performs $T = 5$ refinement iterations under the same inference configuration while maintaining a fixed-width population. For PRISM, we use temperature $T_{\text{smc}} = 0.8$, ESS threshold $\alpha = 0.5$, noise $\eta = 0.1$, clamp $c = 0.3$, clone cap $\kappa = 0.3$. All baselines are implemented within our codebase for consistency, following their official source code and configuration details (if any) as closely as possible. `gpt-oss` models use the medium reasoning effort setting, while Qwen models are limited by a 32K token context window by default.

4.5 Evaluation metrics

In addition to final accuracy, we evaluate inference behavior using population-level and compute-aware metrics.

Population accuracy: At each refinement depth t , each candidate $\tau_{q,i}^{(t)}$ yields an extracted answer $\text{Ans}(\tau_{q,i}^{(t)})$. We measure the fraction of correct candidates:

$$\text{PopAcc}(t) = \mathbb{E}_{q \sim \mathcal{D}} \left[\frac{1}{N} \sum_{i=1}^N \mathbf{1}\{\text{Ans}(\tau_{q,i}^{(t)}) = y_q\} \right], \quad (5)$$

which captures whether refinement increases the density of correct candidates.

NetFlip: To separate genuine correction from “random-walk” rewriting, we measure directional correctness change between consecutive refinement steps. Let $I2C(t)$ be the number of incorrect→correct transitions and $C2I(t)$ the number of correct→incorrect transitions from step $t-1$ to t . We define

$$\text{NetFlip} = \sum_{t \in T} (I2C(t) - C2I(t)) \quad (6)$$

Positive values indicate net error correction, while negative values indicate net degradation.

Compute: We report compute as total token usage across all model calls during inference (including generation, verification, and comparison) and analyze accuracy–compute tradeoffs across methods. We also report estimated cost for relative comparison under a fixed pricing assumption (see Table 1).

5 Results and discussion

We evaluate the effectiveness of PRISM under controlled settings and analyze how it translates inference-time compute into reasoning performance. We compare against state-of-the-art DEEP THINK baselines, examine compute–accuracy tradeoffs, and study refinement dynamics and robustness. Across reasoning benchmarks, PRISM consistently improves final accuracy over both lightweight and refinement-heavy baselines, enabling a 20B model to match or exceed a 120B zero-shot baseline. PRISM also converts additional compute into gains efficiently, frequently lying on the compute–accuracy Pareto frontier where several refinement-heavy methods fail to outperform simple majority voting. Finally, PRISM exhibits stable upward population dynamics, produces consistent directional error correction, improves robustness under weak or noisy initial populations, and yields more reliable aggregation. We detail these findings below.

5.1 Accuracy and compute efficiency

PRISM consistently improves final accuracy while remaining on or near the compute–accuracy Pareto frontier: Table 1 reports final accuracy across methods under matched inference configuration. Across all datasets, PRISM is competitive with or exceeds strong DEEP THINK baselines while maintaining comparable compute.

⁴Estimated cost is computed from the total token usage across all datasets, assuming a 60/40 input/output split. Input and output tokens are priced at \$0.05 and \$0.20 per million tokens (<https://www.together.ai/>). Values are shown for relative comparison, since absolute cost depends on the provider and the input/output ratio. See Section 5.3 for our experiments with Qwen3.

Table 1: Across mathematics and science benchmarks, PRISM is competitive with or outperforms strong DEEPTHINK baselines while maintaining comparable compute. ⁴

Method	Aggregation	AIME25	HMMT25	GPQA Diamond	Cost (\$)
<i>Non-DEEPTHINK baselines</i>					
gpt-oss-120b (zero-shot)	–	77.8	68.9	69.7	0.20
gpt-oss-20b (zero-shot)	–	58.9	44.4	59.7	0.08
Majority Vote	Majority Vote	76.6	58.9	65.8	0.87
<i>DEEPTHINK baselines + Majority Vote</i>					
SciMaster	Majority Vote	84.4	70.0	63.4	6.60
Agentic Debate	Majority Vote	85.6	72.2	65.0	4.67
MAD Conformist	Majority Vote	81.1	66.7	66.9	1.71
MAD Follower	Majority Vote	80.0	62.2	64.7	3.30
Recursive Self-Aggregation	Majority Vote	87.8	77.8	68.6	4.03
<i>DEEPTHINK baselines + LLM Aggregate</i>					
SciMaster	LLM Aggregate	77.8	70.0	63.9	6.87
Agentic Debate	LLM Aggregate	82.2	75.6	58.1	4.80
MAD Conformist	LLM Aggregate	82.2	65.6	63.6	1.81
MAD Follower	LLM Aggregate	83.3	73.3	63.3	3.4
Recursive Self-Aggregation	LLM Aggregate	84.4	74.4	64.7	4.15
<i>Our methods</i>					
PRM-score Vote	PRM-score Vote	77.8	59.7	64.7	1.01
PRISM	Majority Vote	87.8	72.2	71.7	6.76
PRISM	LLM Aggregate	86.7	75.6	68.3	7.11
PRISM	PRM-score Vote	90.0	75.4	71.4	6.76

On AIME25, PRISM with PRM-score voting achieves 90.0%, surpassing Recursive Self-Aggregation (87.8%) and Agentic Debate (85.6%). On HMMT, PRISM reaches 75.4%, remaining competitive with debate-based and aggregation-heavy methods. On GPQA Diamond, PRISM attains 71.4%, improving over Recursive Self-Aggregation (68.6%) and all majority-driven approaches. Notably, PRISM enables gpt-oss-20B to match or outperform gpt-oss-120B, which shows that improved inference can substitute for larger model size.

Figure 3 presents the compute-accuracy frontier on GPQA. Many refinement-heavy baselines lie inside the Pareto region, spending substantially more tokens for marginal or inconsistent gains, whereas PRISM consistently lies on or near the frontier, indicating more efficient conversion of compute into accuracy.

A key observation is that Majority Vote is already a strong baseline, reaching 65.8% on GPQA. Several refinement-heavy methods fail to surpass it despite higher token usage, which suggests that iterative rewriting without a correctness signal often changes answers without reliably improving them. PRISM avoids this inefficiency through step-level verification that guides refinement toward higher-quality reasoning.

5.2 Diagnosing refinement dynamics

We next analyze population-level dynamics to understand why additional refinement compute often fails to translate into correctness.

PRISM makes refinement directionally corrective: Figure 4 shows population accuracy as a function of refinement depth. Across most non-PRM-based methods, population quality oscillates or degrades rather than improving monotonically, which indicates that refinement updates behave

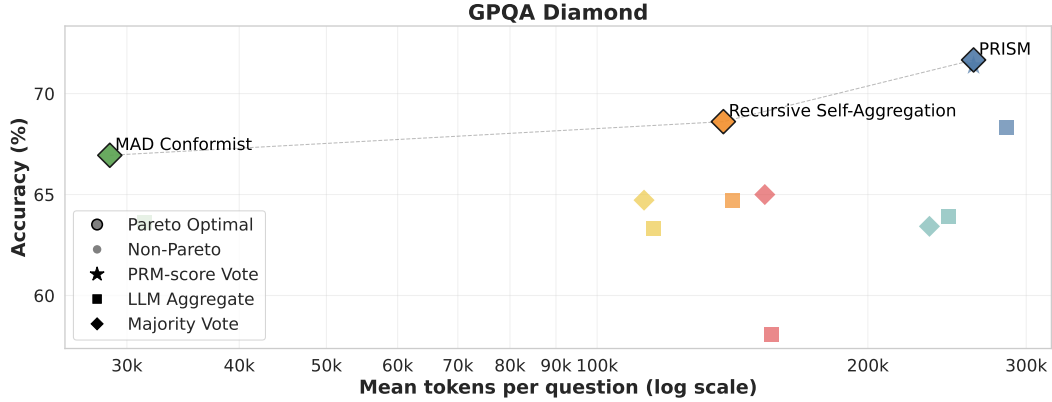


Figure 3: **Compute–accuracy tradeoff on GPQA Diamond (Pareto view)**. Each point represents a method configuration (enhancement + aggregation). The connected frontier marks Pareto-optimal configurations. Most refinement-heavy methods spend substantially more tokens for marginal or inconsistent gains, whereas PRISM stays among the best accuracy-to-compute tradeoffs.

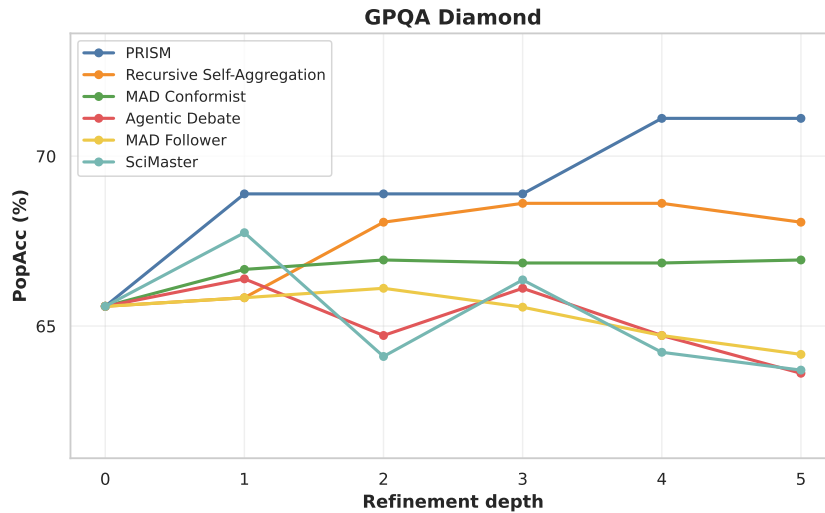


Figure 4: **Population quality vs. refinement depth on GPQA Diamond**. Non-PRM-based methods often oscillate or degrade with depth, whereas PRISM exhibits stable upward population dynamics.

largely as stochastic perturbations rather than directional improvements. In contrast, PRISM shows stable upward population dynamics, which suggests that PRM-guided acceptance filtering suppresses harmful updates and preserves correct trajectories.

To assess whether refinement corrects more errors than it introduces, we measure NetFlip. On GPQA Diamond, most baselines exhibit small positive net flip, which suggests limited directional correction (Figure 5). In many cases, correct trajectories are degraded nearly as often as incorrect ones are repaired. In contrast, PRISM produces substantially larger positive NetFlip values, which shows that refinement is more consistently aligned with correctness.

PRISM preserves correct minority solutions and remains robust in low-correctness regimes:

To examine how different methods behave under varying initial population quality, we group instances by the number of correct candidates present in the initial population before refinement and report final accuracy within each group using majority voting for all methods. We visualize our results on GPQA Diamond in Figure 6.

Majority-driven refinement (e.g., MAD Conformist/Follower) stabilizes populations by anchoring candidates to frequent solutions. However, this induces a structural failure mode in which correct

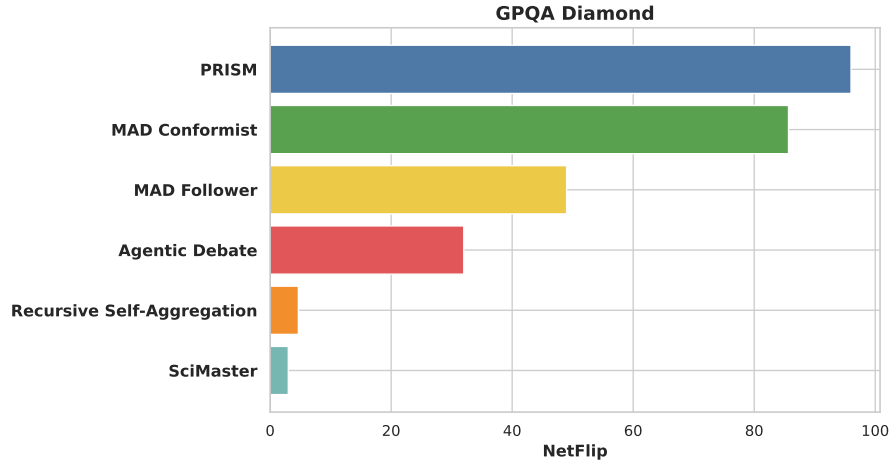


Figure 5: **Directional correction across enhancement depth on GPQA Diamond.** Bars show NetFlip aggregated over depth and averaged across questions. Positive values indicate more incorrect→correct than correct→incorrect transitions, reflecting genuine correction rather than “random-walk” reshuffling.

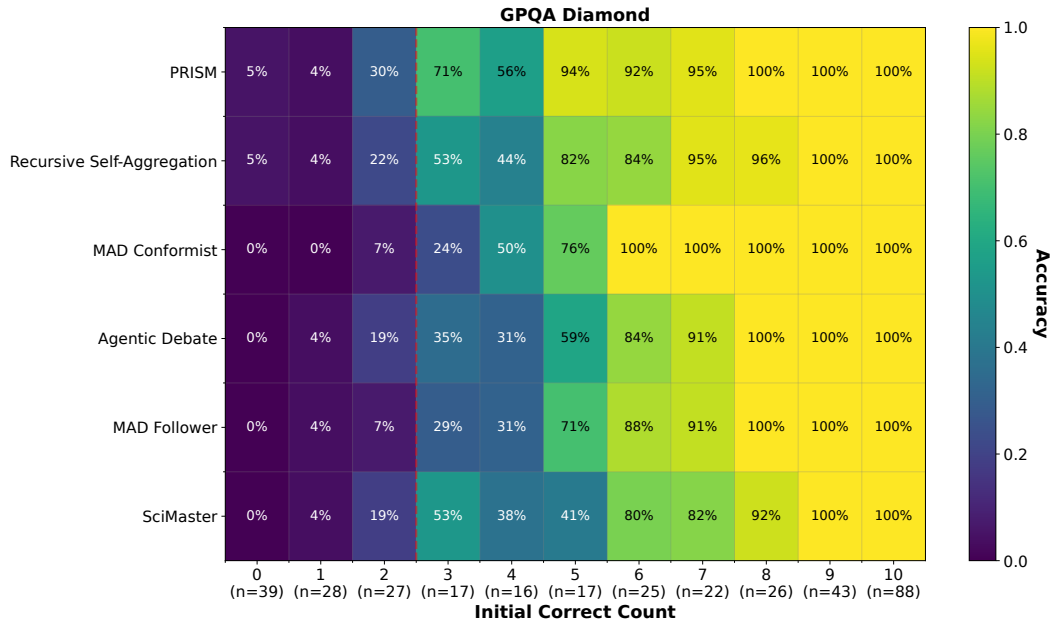


Figure 6: **GPQA performance conditioned on initial population quality.** Each column groups problems by how many correct solutions appear in the initial candidate pool, and each cell reports the final accuracy after refinement and majority voting. While most methods struggle when few correct candidates are present at the start, PRISM maintains substantially higher accuracy in these low-correctness regimes, which shows stronger resilience to weak initial populations.

minority trajectories are suppressed by more frequent but incorrect reasoning. When the initial majority is wrong, consensus-based dynamics drive the population toward a confident but incorrect answer. This effect is most pronounced in low-correctness regimes, where these methods rarely recover once incorrect reasoning becomes dominant.

In contrast, PRISM degrades substantially less in low-correctness bins. Even when the initial population contains few correct candidates, PRISM achieves markedly higher final accuracy than competing methods. This indicates that PRISM can “bootstrap” from weak populations rather than simply amplifying the dominant trajectory. This behavior aligns with PRISM’s refinement mechanism.

Table 2: **Resampling dynamics.** $t = 0$ is initialization; $t = 4$ is after four refinement steps. $ESS/N \in [0, 1]$ measures weight concentration (higher means more evenly distributed weights). Resampling rate is the fraction of iterations that triggered resampling. Dominance rate w/o clone cap (%) reports the probability that a single candidate exceeds 30% of the next generation ($P(max > 0.3)$) and the probability of full takeover ($P(max = 1)$).

Dataset	ESS/N		Resampling rate		Dominance rate w/o clone cap	
	$t=0$	$t=4$	$t=0$	$t=4$	$P(max > 0.3)$	$P(max = 1)$
AIME	0.282	0.879	0.756	0.033	0.854	0.282
HMMT	0.237	0.812	0.795	0.085	0.768	0.134
GPQA	0.333	0.838	0.503	0.064	0.989	0.316

Table 3: **Proposal acceptance dynamics.** r is the PRM score ratio between the proposal and the current trace. $P(accept|r_s < 1)$ reports the downhill acceptance rate (percentage of lower-scoring proposals that are accepted). $\mathbb{E}[s(\tau') | \text{accepted}]$ and $\mathbb{E}[s(\tau') | \text{rejected}]$ denote the average PRM score of proposed traces when accepted or rejected, respectively. Values are mean across runs with min-max in parentheses.

Dataset	$P(accept r_w < 1)$	$\mathbb{E}[s(\tau') \text{accepted}]$	$\mathbb{E}[s(\tau') \text{rejected}]$
AIME	0.101 (0.094-0.106)	0.794 (0.781-0.805)	0.025 (0.023-0.026)
HMMT	0.179 (0.138-0.238)	0.692 (0.677-0.713)	0.045 (0.031-0.060)
GPQA	0.104 (0.087-0.117)	0.763 (0.756-0.778)	0.023 (0.021-0.024)

As updates are guided by step-level correctness signals rather than frequency, promising minority trajectories are less likely to be overwritten. As a result, PRISM avoids majority dilution and maintains recovery capacity when correct reasoning is initially rare.

Directional refinement makes aggregation more reliable: Aggregation quality depends on the refined population. For most baselines, switching from majority vote to LLM aggregation often reduces accuracy, which suggests that the aggregator can rationalize confident but incorrect traces when the population is noisy (see Table 1). In contrast, PRISM maintains stable performance under LLM aggregation, indicating that directional refinement produces more accurate and internally consistent populations. PRM-score voting further mitigates majority dilution when correct answers are rare (e.g., on AIME), while having little effect when refinement already promotes correct trajectories into the majority (e.g., on GPQA).

Directional refinement and population stabilization in PRISM: We now examine PRISM’s internal refinement dynamics. At each iteration t , PRISM assigns PRM-based weights to candidate traces and triggers resampling when weight concentration becomes severe, which is tracked by normalized ESS/N (higher indicates greater population diversity, i.e., more evenly distributed weights). As shown in Table 2, early refinement exhibits strong weight concentration ($ESS/N \approx 0.24-0.33$), which triggers frequent resampling (50.3%–79.5%). By $t = 4$, ESS/N rises to 0.81-0.88 and resampling drops to 3.3%–8.5%, indicating stabilization of the candidate pool. Without clone capping, a single trajectory would often exceed a 30% share of the population ($P(max > 0.3)$) and full takeover ($P(max = 1)$) would occur non-trivially. The clone cap prevents such collapse and preserves diversity needed for reliable aggregation and recovery.

After resampling, PRISM proposes stochastic updates to candidate solutions, and accepts or rejects each proposal based on the score ratio r_s . Table 3 shows that accepted proposals consistently receive higher PRM scores than rejected ones, and score-decreasing proposals (downhill moves) are still accepted with non-zero probability (0.101-0.179), which preserves exploration. The number of accepted proposals correlates positively with improvements in population correctness on AIME and GPQA ($r = 0.152$ and 0.172), while remaining weaker on HMMT ($r = 0.023$), suggesting that the PRM provides a useful, though imperfect, local signal, while PRM’s acceptance rule still maintains exploration through occasional lower-scoring updates.

5.3 Experiments with Qwen3 model family

PRISM generalizes across models and benefits from stronger verifiers: Across AIME, HMMT, and GPQA, PRISM consistently improves over the zero-shot baseline, with the largest gains observed on smaller models (Figures 15–17) in Appendix D. Although PRISM incurs additional inference-time

compute, it remains competitive on the accuracy–compute Pareto frontier under Qwen3 (Figures 18–20), which suggests that improvements arise from more effective compute allocation rather than increased token usage alone. We further probe the role of verifier strength by pairing Qwen3 generators and verifiers of different sizes. Figure 21 shows that PRISM benefits most when the verifier is stronger than the generator (e.g., a 1.7B generator paired with 14B or 30B verifiers). Finally, to assess robustness across model variants, we apply PRISM to Qwen-4B Base, Instruct, and Thinking. Across datasets, PRISM produces larger gains for weaker variants (e.g., base) and substantially narrows the gap to stronger models (e.g., thinking).

6 Related work

Test-time scaling and DEEPTHINK frameworks: A growing line of work studies how additional inference-time compute can trade off with pretraining compute to improve reasoning performance. Broadly, these approaches scale reasoning along two axes. *Sequential scaling* generates solution attempts iteratively, where later attempts condition on earlier ones so that the model extends and refines its reasoning [Snell et al., 2025, Muennighoff et al., 2025]. For example, Muennighoff et al. [2025] rely on budget forcing, which artificially truncates or extends reasoning chains to control compute allocation. In contrast, *parallel scaling* generates multiple solution attempts concurrently and selects among them, for example, by using majority voting or Best-of-N strategies [Snell et al., 2025, Brown et al., 2025]. Hybrid approaches combine sequential reasoning with parallel exploration, which includes tree-based inference methods such as Monte Carlo Tree Search [Zhang et al., 2023, Zhou et al., 2024] and guided beam search [Xie et al., 2023], as well as approaches that incorporate process-level rewards to guide sequential search [Wu et al., 2025].

Our work situates itself within the emerging class of DEEPTHINK frameworks, which extends the parallel paradigm by synergistically refining and combining interdependent reasoning paths rather than treating candidates as independent samples [Google, 2025, 2026, Fu et al., 2026, Dong et al., 2026]. Methods such as SciMaster [Chai et al., 2025] and Recursive Self-Aggregation [Venkatraman et al., 2025] rely on iterative refinement and structured aggregation to progressively improve candidate solutions. In contrast, approaches like Agentic Debate [Wang et al., 2025] and MAD Conformist/Follower [Choi et al., 2025] emphasize agentic interaction and majority-driven consensus to coordinate reasoning across candidates. In this work, we introduce a functional taxonomy of DEEPTHINK that decomposes existing frameworks into population creation, enhancement, and aggregation, and we identify a refinement bottleneck that limits accuracy and compute efficiency. PRISM addresses this bottleneck by integrating step-level correctness signals directly into inference, which enables directional population updates rather than stochastic rewriting or purely majority-driven selection.

Process reward modeling: Process reward models (PRMs) provide step-level supervision over intermediate reasoning steps rather than only final answers [Lightman et al., 2024]. Prior work has primarily used PRM outputs as evaluative signals for ranking, filtering, or reinforcement learning, where they score completed trajectories and guide training or selection [Wang et al., 2024, Wu et al., 2025]. In contrast, PRISM interprets PRM scores as defining an implicit energy landscape over reasoning trajectories. These scores shape population dynamics through resampling and stochastic refinement, converting step-level correctness signals into directional inference updates that move the population toward lower-energy, higher-quality regions. By embedding PRM scores directly into refinement, PRISM transforms evaluation into structured population optimization.

7 Conclusion

We introduced a functional taxonomy of DEEPTHINK systems and identified population enhancement as the key bottleneck that limits the effective use of inference-time compute. To address this limitation, we proposed PRISM, a Process Reward Model (PRM)-guided inference algorithm that embeds step-level correctness signals directly into refinement and aggregation. By interpreting PRM scores as defining an implicit energy landscape over reasoning trajectories, PRISM converts iterative refinement from stochastic rewriting into directional population optimization. Across mathematical and scientific benchmarks, PRISM consistently improves accuracy, produces stable directional correction, remains robust in low-correctness regimes, and frequently lies on the compute-accuracy Pareto frontier. These results indicate that reliable step-level verification is a key ingredient for scalable inference-time reasoning. More broadly, our findings highlight the importance of correctness-sensitive refinement mechanisms for building principled, efficient, and robust DEEPTHINK systems.

8 Limitations

Our conclusions should be viewed in light of several design choices that constrain the scope of this study.

PRM instantiation: PRISM depends on a step-level scalar signal to shape refinement and aggregation. In our experiments, the PRM is instantiated as a prompted model derived from the same base LLM and executed deterministically. This setup allows us to isolate the effect of PRM-guided population dynamics in a controlled setting, but it represents only one possible realization of the framework. In domains where stronger or externally grounded feedback is available, such as executable tests or formal verification tools, the scoring signal could be substantially more reliable. Therefore, our results demonstrate the effectiveness of integrating step-level signals into inference, but they do not fully characterize performance under richer reward sources.

Step segmentation: PRISM assumes that reasoning can be decomposed into meaningful steps. When segmentation does not align with coherent logical units, step-level scoring may be less informative, which weakens refinement guidance. Improved segmentation or more structured reasoning representations could further enhance the effectiveness of step-level signals.

References

- Sandhini Agarwal, Lama Ahmad, Jason Ai, Sam Altman, Andy Applebaum, Edwin Arbus, Rahul K Arora, Yu Bai, Bowen Baker, Haiming Bao, et al. gpt-oss-120b & gpt-oss-20b model card. *arXiv preprint arXiv:2508.10925*, 2025. URL <https://arxiv.org/abs/2508.10925>.
- Mislav Balunovic, Jasper Dekoninck, Ivo Petrov, Nikola Jovanović, and Martin Vechev. Matharena: Evaluating LLMs on uncontaminated math competitions. In *The Thirty-ninth Annual Conference on Neural Information Processing Systems Datasets and Benchmarks Track*, 2025. URL <https://openreview.net/forum?id=y0zL9IZxZ7>.
- Bradley Brown, Jordan Juravsky, Ryan Saul Ehrlich, Ronald Clark, Quoc V Le, Christopher Re, and Azalia Mirhoseini. Large language monkeys: Scaling inference compute with repeated sampling, 2025. URL <https://openreview.net/forum?id=0xUEBQV54B>.
- Jingyi Chai, Shuo Tang, Rui Ye, Yuwen Du, Xinyu Zhu, Mengcheng Zhou, Yanfeng Wang, Yuzhi Zhang, Linfeng Zhang, Siheng Chen, et al. Scimaster: Towards general-purpose scientific ai agents, part i. x-master as foundation: Can we lead on humanity’s last exam? *arXiv preprint arXiv:2507.05241*, 2025. URL <https://arxiv.org/abs/2507.05241>.
- Hyeong Kyu Choi, Jerry Zhu, and Sharon Li. Debate or vote: Which yields better decisions in multi-agent large language models? In *The Thirty-ninth Annual Conference on Neural Information Processing Systems*, 2025. URL <https://openreview.net/forum?id=iUjGNJzrF1>.
- Harry Dong, David Brandfonbrener, Eryk Helenowski, Yun He, Mrinal Kumar, Han Fang, Yuejie Chi, and Karthik Abinav Sankararaman. Generalized parallel scaling with interdependent generations. In *The Fourteenth International Conference on Learning Representations*, 2026. URL <https://openreview.net/forum?id=suU6kAP6c2>.
- Yichao Fu, Xuwei Wang, Hao Zhang, Yuandong Tian, and Jiawei Zhao. Deep think with confidence. In *The Fourteenth International Conference on Learning Representations*, 2026. URL <https://openreview.net/forum?id=8LqHsOKIM7>.
- Google. Try deep think in the gemini app. 2025. URL <https://blog.google/products-and-platforms/products/gemini/gemini-2-5-deep-think/>.
- Google. Gemini 3 deep think: Advancing science, research and engineering. 2026. URL <https://blog.google/innovation-and-ai/models-and-research/gemini-models/gemini-3-deep-think/>.
- Ari Holtzman, Jan Buys, Li Du, Maxwell Forbes, and Yejin Choi. The curious case of neural text degeneration. In *International Conference on Learning Representations*, 2020. URL <https://openreview.net/forum?id=rygGQyrFvH>.
- Hunter Lightman, Vineet Kosaraju, Yuri Burda, Harrison Edwards, Bowen Baker, Teddy Lee, Jan Leike, John Schulman, Ilya Sutskever, and Karl Cobbe. Let’s verify step by step. In *The Twelfth International Conference on Learning Representations*, 2024. URL <https://openreview.net/forum?id=v8L0pN6E0i>.
- Hanzhao (Maggie) Lin and Heng-Tze Cheng. Gemini achieves gold-medal level at the international collegiate programming contest world finals. 2025. URL <https://deepmind.google/blog/gemini-achieves-gold-medal-level-at-the-international-collegiate-programming-contest-world-finals/>.
- Thang Luong and Edward Lockhart. Advanced version of gemini with deep think officially achieves gold-medal standard at the international mathematical olympiad. 2025. URL <https://deepmind.google/blog/advanced-version-of-gemini-with-deep-think-officially-achieves-gold-medal-standard-at-the-international-mathematical-olympiad/>.
- Thang Luong and Vahab Mirrokni. Accelerating mathematical and scientific discovery with gemini deep think. 2026. URL <https://deepmind.google/blog/accelerating-mathematical-and-scientific-discovery-with-gemini-deep-think/>.

- Niklas Muennighoff, Zitong Yang, Weijia Shi, Xiang Lisa Li, Li Fei-Fei, Hannaneh Hajishirzi, Luke Zettlemoyer, Percy Liang, Emmanuel Candes, and Tatsunori Hashimoto. s1: Simple test-time scaling. In Christos Christodoulopoulos, Tanmoy Chakraborty, Carolyn Rose, and Violet Peng, editors, *Proceedings of the 2025 Conference on Empirical Methods in Natural Language Processing*, pages 20275–20321, Suzhou, China, November 2025. Association for Computational Linguistics. ISBN 979-8-89176-332-6. doi: 10.18653/v1/2025.emnlp-main.1025. URL <https://aclanthology.org/2025.emnlp-main.1025/>.
- Long Phan, Arunim Agarwal, and Dan Hendrycks. Cais ai dashboard. <https://dashboard.safe.ai>, 2025.
- David Rein, Betty Li Hou, Asa Cooper Stickland, Jackson Petty, Richard Yuanzhe Pang, Julien Dirani, Julian Michael, and Samuel R. Bowman. GPQA: A graduate-level google-proof q&a benchmark. In *First Conference on Language Modeling*, 2024. URL <https://openreview.net/forum?id=Ti67584b98>.
- Charlie Victor Snell, Jaehoon Lee, Kelvin Xu, and Aviral Kumar. Scaling LLM test-time compute optimally can be more effective than scaling parameters for reasoning. In *The Thirteenth International Conference on Learning Representations*, 2025. URL <https://openreview.net/forum?id=4FWAwZtd2n>.
- Siddarth Venkatraman, Vineet Jain, Sarthak Mittal, Vedant Shah, Johan Obando-Ceron, Yoshua Bengio, Brian R Bartoldson, Bhavya Kailkhura, Guillaume Lajoie, Glen Berseth, et al. Recursive self-aggregation unlocks deep thinking in large language models. *arXiv preprint arXiv:2509.26626*, 2025. URL <https://arxiv.org/abs/2509.26626>.
- Han Wang, Archiki Prasad, Elias Stengel-Eskin, and Mohit Bansal. Retrieval-augmented generation with conflicting evidence. In *Second Conference on Language Modeling*, 2025. URL <https://openreview.net/forum?id=z1MHB2m3V9>.
- Peiyi Wang, Lei Li, Zhihong Shao, Runxin Xu, Damai Dai, Yifei Li, Deli Chen, Yu Wu, and Zhifang Sui. Math-shepherd: Verify and reinforce LLMs step-by-step without human annotations. In Lun-Wei Ku, Andre Martins, and Vivek Srikumar, editors, *Proceedings of the 62nd Annual Meeting of the Association for Computational Linguistics (Volume 1: Long Papers)*, pages 9426–9439, Bangkok, Thailand, August 2024. Association for Computational Linguistics. doi: 10.18653/v1/2024.acl-long.510. URL <https://aclanthology.org/2024.acl-long.510/>.
- Xuezhi Wang, Jason Wei, Dale Schuurmans, Quoc V Le, Ed H. Chi, Sharan Narang, Aakanksha Chowdhery, and Denny Zhou. Self-consistency improves chain of thought reasoning in language models. In *The Eleventh International Conference on Learning Representations*, 2023. URL <https://openreview.net/forum?id=1PL1NIMMrw>.
- Yangzhen Wu, Zhiqing Sun, Shanda Li, Sean Welleck, and Yiming Yang. Inference scaling laws: An empirical analysis of compute-optimal inference for LLM problem-solving. In *The Thirteenth International Conference on Learning Representations*, 2025. URL <https://openreview.net/forum?id=VNckp7JEHn>.
- Yuxi Xie, Kenji Kawaguchi, Yiran Zhao, Xu Zhao, Min-Yen Kan, Junxian He, and Qizhe Xie. Self-evaluation guided beam search for reasoning. In *Thirty-seventh Conference on Neural Information Processing Systems*, 2023. URL <https://openreview.net/forum?id=Bw82hwg5Q3>.
- An Yang, Anfeng Li, Baosong Yang, Beichen Zhang, Binyuan Hui, Bo Zheng, Bowen Yu, Chang Gao, Chengen Huang, Chenxu Lv, et al. Qwen3 technical report. *arXiv preprint arXiv:2505.09388*, 2025. URL <https://arxiv.org/abs/2505.09388>.
- Jiayi Zhang, Simon Yu, Derek Chong, Anthony Sicilia, Michael R Tomz, Christopher D Manning, and Weiyang Shi. Verbalized sampling: How to mitigate mode collapse and unlock llm diversity. *arXiv preprint arXiv:2510.01171*, 2025. URL <https://arxiv.org/abs/2510.01171>.
- Shun Zhang, Zhenfang Chen, Yikang Shen, Mingyu Ding, Joshua B. Tenenbaum, and Chuang Gan. Planning with large language models for code generation. In *The Eleventh International Conference on Learning Representations*, 2023. URL <https://openreview.net/forum?id=Lr8c00tYbfL>.

Andy Zhou, Kai Yan, Michal Shlapentokh-Rothman, Haohan Wang, and Yu-Xiong Wang. Language agent tree search unifies reasoning, acting, and planning in language models. In *Forty-first International Conference on Machine Learning*, 2024. URL <https://openreview.net/forum?id=njwv9BsGHF>.

A Step verifier and score construction

A.1 Step verifier prompt

We instantiate the verifier V as a prompted auditor model that produces step-level judgments in $\{+1, 0, -1\}$ plus a FINAL ANSWER CHECK. The verifier is run deterministically (temperature 0) to reduce variance across refinement iterations.

Input formatting: Given a candidate trace τ , we segment the reasoning into an ordered sequence of steps and wrap each step in a `<step i="k">...</step>` tag (1-indexed). The verifier input consists of: (i) the problem statement, (ii) the tagged step sequence, and (iii) the proposed final answer.

Output schema: The verifier must return exactly one line per input step (in the same order), each containing a brief note and a trailing score token in $\{+1, 0, -1\}$, followed by a FINAL ANSWER CHECK line with a token in $\{+1, 0, -1\}$. We parse only the score tokens and ignore free-form notes.

```
[SYSTEM_PROMPT]
You are a strict auditor. Find the earliest mistake.
Input: Problem, Steps (<step>...</step>), Proposed Answer.
RULES:
1) Judge EACH step independently (logic + math + consistency with Problem).
2) If a step is wrong, mark it -1. Any later step that depends on it is -1.
3) If a step is correct but trivial/doesn't advance the solution, mark 0.
4) If anything is missing/ambiguous/unverifiable, mark -1.
5) Be skeptical of 'clean' answers when derivation is not fully justified.
OUTPUT (STRICT):
Return EXACTLY one line per input step, in the SAME ORDER.
Do NOT copy the original step text.
Each line MUST be:
  <step i="k">note <= 12 words ... +1|0|-1</step>
The score token MUST be inside the <step ...> tag at the end.
Do NOT put anything after </step>.
Do NOT output the literal string '+1|0|-1' (choose exactly one).
Example OK:
  <step i="1">Algebra correct +1</step>
Example NOT OK:
  <step i="1">Algebra correct</step> +1
  <step i="1">Algebra correct +1|0|-1</step>
Use i="1" for the first input step, i="2" for the second, etc.
After these, output exactly one final line:
  <step>FINAL ANSWER CHECK: +1|0|-1</step>
FINAL ANSWER CHECK = -1 if Proposed Answer is wrong or not the requested
quantity.
FINAL ANSWER CHECK = 0 if cannot verify but might be correct.
FINAL ANSWER CHECK = +1 only if it is clearly correct.
Then output exactly one line:
  <answer>+1</answer> iff (all steps are +1) AND (FINAL ANSWER CHECK is +1).
  <answer>-1</answer> otherwise.
[USER_PROMPT]
Problem: {question}
Reasoning: {answer.reasoning}
Proposed Answer: {answer.choice}
Follow the system instructions exactly. Output only <step> lines and the final <
answer> line.
```

A.2 Parsing and failure handling

Verifier outputs are treated as structured text. A verifier call is considered successful if it: (i) emits one parsable score token for every non-final step, (ii) uses only tokens in $\{+1, 0, -1\}$, and (iii) emits a parsable FINAL ANSWER CHECK token.

Any violation (e.g., missing lines, malformed tags, out-of-range tokens, or parsing-breaking extra text) is treated as VERIFICATION_FAILED, and the trace receives the fixed fallback score specified in Section A.3. (We clamp scores to a small $\epsilon > 0$ before forming ratios/weights to avoid division-by-zero in acceptance computations.)

A.3 Scoring, particle weights, and acceptance

For each trace τ , we compute a scalar verifier score $s(\tau) \in [0, 1]$ from the parsed feedback.

Step ratio: Let $n_{\text{correct}}, n_{\text{neutral}}, n_{\text{incorrect}}$ be the counts of +1, 0, -1 labels over non-final steps (excluding FINAL ANSWER CHECK). We define

$$\text{step_ratio} = \frac{n_{\text{correct}} + 0.5 n_{\text{neutral}}}{n_{\text{correct}} + n_{\text{neutral}} + n_{\text{incorrect}}}.$$

This weighted average treats correct steps as full credit, incorrect steps as no credit, and neutral steps as partial credit. The partial weight mitigates penalties on long traces where neutral labels are common, while still separating clean reasoning from clearly incorrect reasoning.

Final verdict: The FINAL ANSWER CHECK token yields the final verdict: CORRECT (+1), INCORRECT (-1), or NEUTRAL (0). If the final line is missing but step parsing succeeded, we mark it as MISSING. If parsing fails, we mark VERIFICATION_FAILED.

Scalar PRM score: The verifier provides two complementary signals: (i) *how clean the reasoning is* (captured by step_ratio) and (ii) *whether the final answer is actually correct* (captured by the final verdict v). We combine them so that step-level quality can refine rankings *within* a verdict class, but cannot override the final correctness signal.

Concretely, we map step_ratio to a scalar score using a verdict-dependent affine transform

$$s(\tau) = a_v + b_v \cdot \text{step_ratio}.$$

If $v = \text{INCORRECT}$, we cap the score below 0.3 so a wrong final answer cannot achieve a high score even if intermediate steps look plausible. If $v = \text{CORRECT}$, we floor the score at 0.5 and scale upward with step_ratio so cleaner reasoning is preferred among correct solutions. Neutral or missing final verdicts receive intermediate scaling to reflect uncertainty.

The parameters are:

$$(a_v, b_v) = \begin{cases} (0, 0.3), & v = \text{INCORRECT} \\ (0.5, 0.5), & v = \text{CORRECT} \\ (0, 0.6), & v = \text{NEUTRAL} \\ (0, 0.8), & v = \text{MISSING} \\ (0, 0), & v = \text{VERIFICATION_FAILED} \end{cases}$$

B Stochastic refinement proposals

B.1 Mixture proposal distribution

The iterator model I proposes refinement moves $\tau \rightarrow \tau'$ using a two-component mixture:

$$q(\tau' | \tau) = (1 - \eta) q_{\text{local}}(\tau' | \tau, \text{PRM}(\tau)) + \eta q_{\text{explore}}(\tau' | x),$$

where x is the original problem instance and $\eta \in [0, 1]$ controls exploration.

Local refinement (q_{local}): I is conditioned on x , the current trace τ , and structured PRM feedback on τ . The prompt instructs minimal edits: fix incorrect steps, preserve correct steps, and output a complete revised trace with an explicit final answer.

Exploration (q_{explore}): I is conditioned primarily on x and is instructed to attempt a qualitatively different approach. This component is intended to reduce mode collapse and introduce new reasoning directions.

Decoding and formatting constraints: Outputs must include an explicit final answer line for deterministic answer extraction. If I produces an unparsable output (e.g., missing final answer), we treat the proposal as a no-op ($\tau' = \tau$).

B.2 Iterator prompt templates

```

Problem:\n{state.question}

Previous reasoning:\n{prev_reasoning}
Previous choice: {particle.answer.choice}

Step-by-step verification:
{feedback_summary}

Refine the solution by fixing any -1 steps.
Maintain +1 steps unless you find a better approach.

Formatting requirements:

- Output ONLY <step>...</step> lines.
- Do NOT include markdown headings, separators, or text outside <step> tags.
- Keep the number of steps small and concise.
- Your LAST step MUST contain the final answer:
<step>The final answer is: \boxed{...}</step>

```

```

Problem:
{state.question}

Solve from scratch. Use a DIFFERENT approach than a standard solution if possible.

Formatting requirements:
- Output ONLY <step>...</step> lines.
- Keep steps concise.
- LAST step MUST be: <step>The final answer is: \boxed{...}</step>

```

C Conflict arbitration

PRM-style verifiers can assign similarly high scores to candidates with different extracted answers. To avoid spending compute on incompatible modes, PRISM invokes an explicit arbitration step using the comparator model C .

C.1 Trigger, verdict parsing, and score clamping

Trigger: Let \mathcal{A} be the set of distinct extracted answers in the population. We trigger arbitration when (i) at least two answers exceed a near-perfect threshold, or (ii) the top answers are in a near-tie.

Comparator output: C outputs exactly one tag: `<verdict>A</verdict>`, `<verdict>B</verdict>`, or `<verdict>NEITHER</verdict>`. Malformed outputs are treated as NEITHER.

Score clamping: Let τ_A, τ_B be the compared traces and $c \in (0, 1)$ be a clamp value. If the verdict is A, we clamp $s(\tau_B) \leftarrow \min(s(\tau_B), c)$ and keep $s(\tau_A)$ unchanged (symmetrically for B); for NEITHER, we clamp both. Since weights depend on scores ($w(\tau) = s(\tau)^{1/T}$), clamping reduces the resampling probability of unresolved conflicts and limits their influence on subsequent refinement.

C.2 Comparator prompt template

```

You are a careful judge. Two solutions to the same problem both claim to be
correct.

```

Compare them and determine which one (if any) is actually correct.

Problem:
{problem}

Solution A (answer: {choice_a}):\n{reasoning_a}

Solution B (answer: {choice_b}):\n{reasoning_b}

Instructions:

1. Check each solution's reasoning and final answer.
2. If Solution A is correct and B is wrong, output: <verdict>A</verdict>
3. If Solution B is correct and A is wrong, output: <verdict>B</verdict>
4. If BOTH are wrong or you cannot determine, output: <verdict>NEITHER</verdict>

Output exactly one <verdict>...</verdict> tag with your decision.

D Additional figures

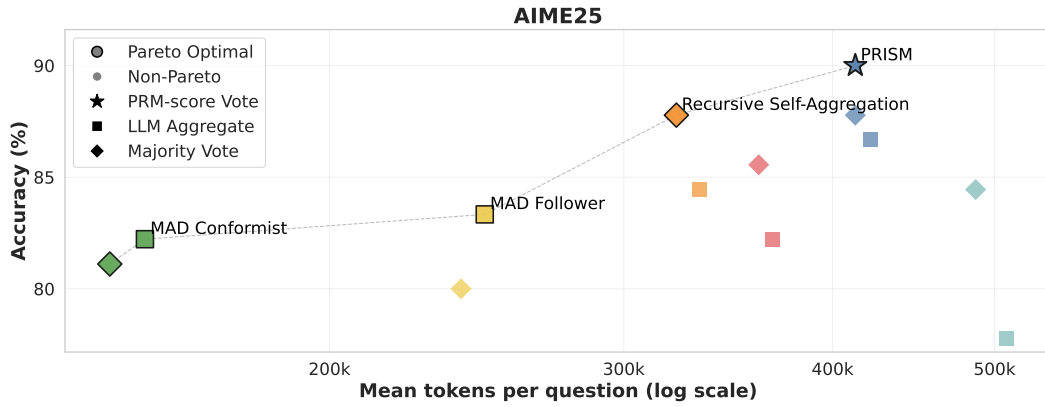


Figure 7: **Compute–accuracy tradeoff on AIME25 (Pareto view)**. Each point represents a method configuration (enhancement + aggregation). The connected frontier marks Pareto-optimal configurations. Most refinement-heavy methods spend substantially more tokens for marginal or inconsistent gains, whereas PRISM stays among the best accuracy-to-compute tradeoffs.

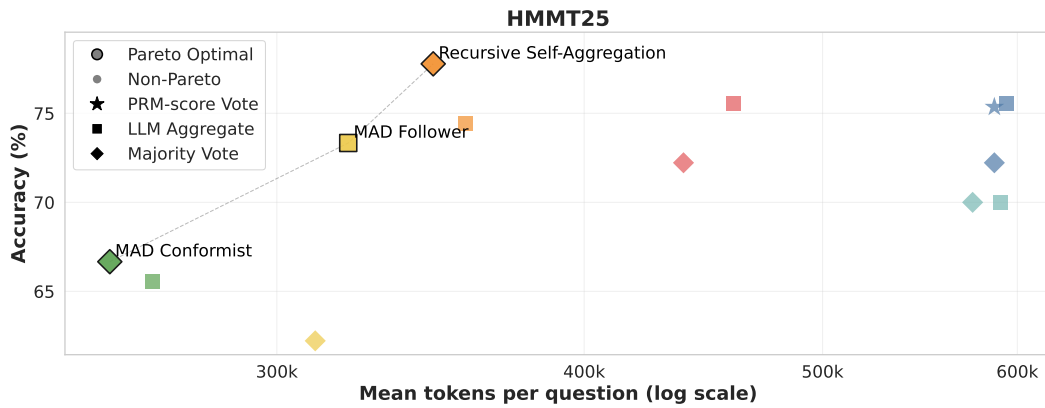


Figure 8: **Compute–accuracy tradeoff on HMMT25 (Pareto view)**. Each point represents a method configuration (enhancement + aggregation). The connected frontier marks Pareto-optimal configurations. Most refinement-heavy methods spend substantially more tokens for marginal or inconsistent gains.

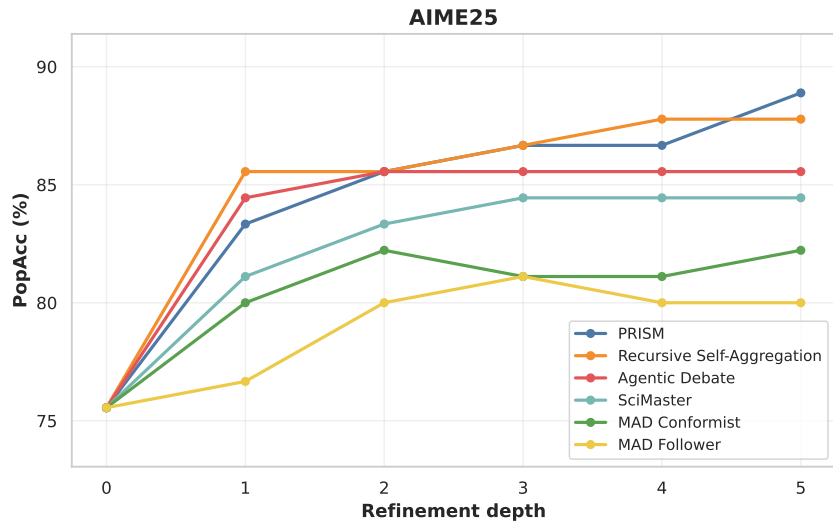


Figure 9: **Population quality vs. refinement depth on AIME25.** Non-PRM-based methods often oscillate or degrade with depth, whereas PRISM exhibits stable upward population dynamics.

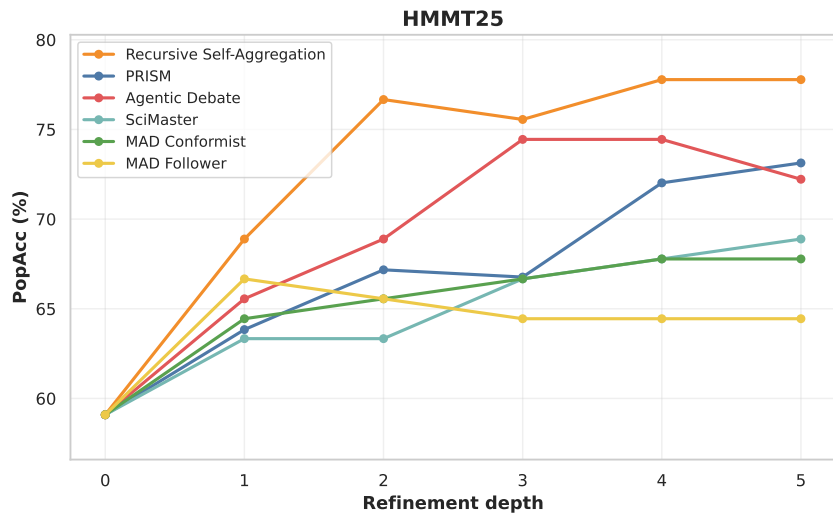


Figure 10: **Population quality vs. refinement depth on HMMT25.** Non-PRM-based methods often oscillate or degrade with depth, whereas PRISM exhibits stable upward population dynamics.

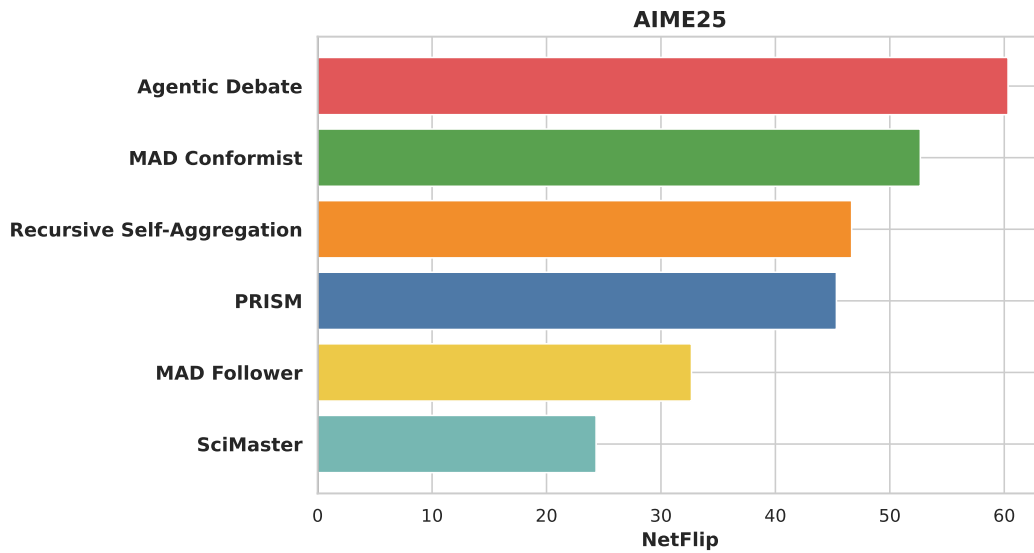


Figure 11: **Directional correction across enhancement depth on AIME25.** Bars show NetFlip aggregated over depth and averaged across questions. Positive values indicate more incorrect→correct than correct→incorrect transitions, reflecting genuine correction rather than “random-walk” reshuffling.

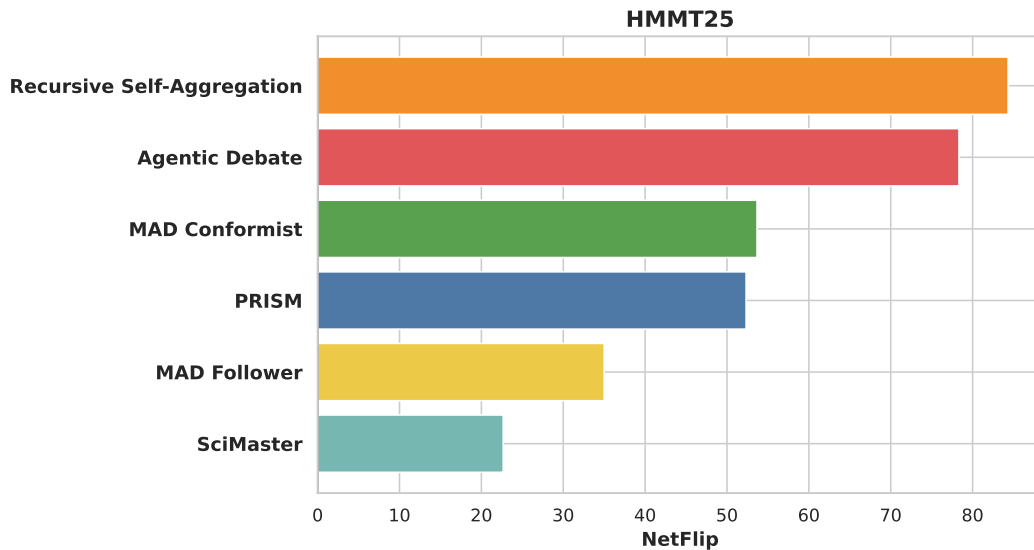


Figure 12: **Directional correction across enhancement depth on HMMT25.** Bars show NetFlip aggregated over depth and averaged across questions. Positive values indicate more incorrect→correct than correct→incorrect transitions, reflecting genuine correction rather than “random-walk” reshuffling.

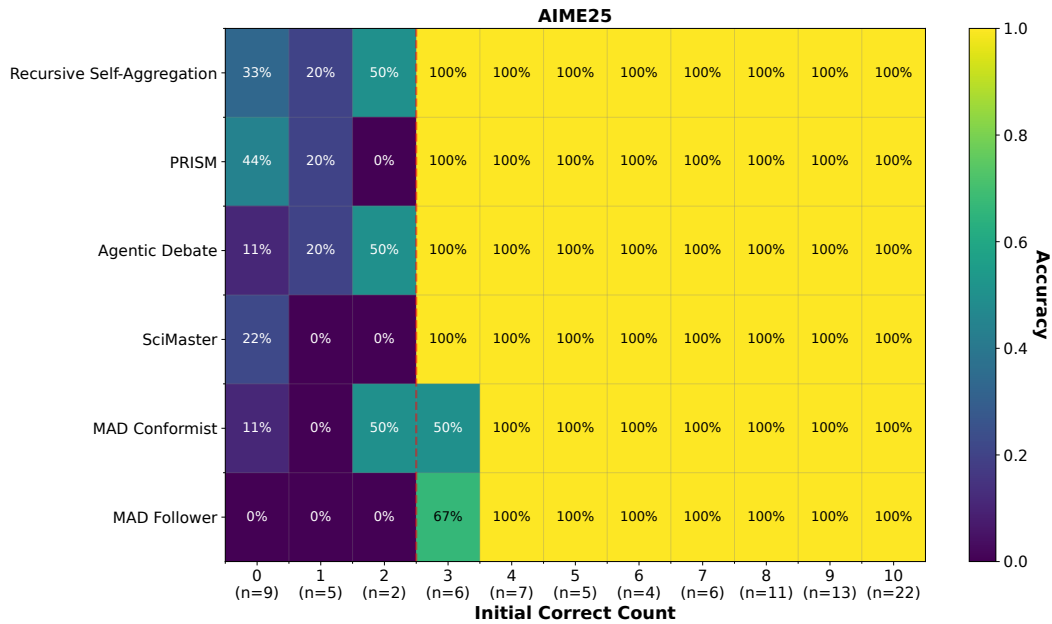


Figure 13: **AIME25 performance conditioned on initial population quality.** Each column groups problems by how many correct solutions appear in the initial candidate pool, and each cell reports the final accuracy after refinement and majority voting. While most methods struggle when few correct candidates are present at the start, PRISM maintains substantially higher accuracy in these low-correctness regimes, which shows stronger resilience to weak initial populations.

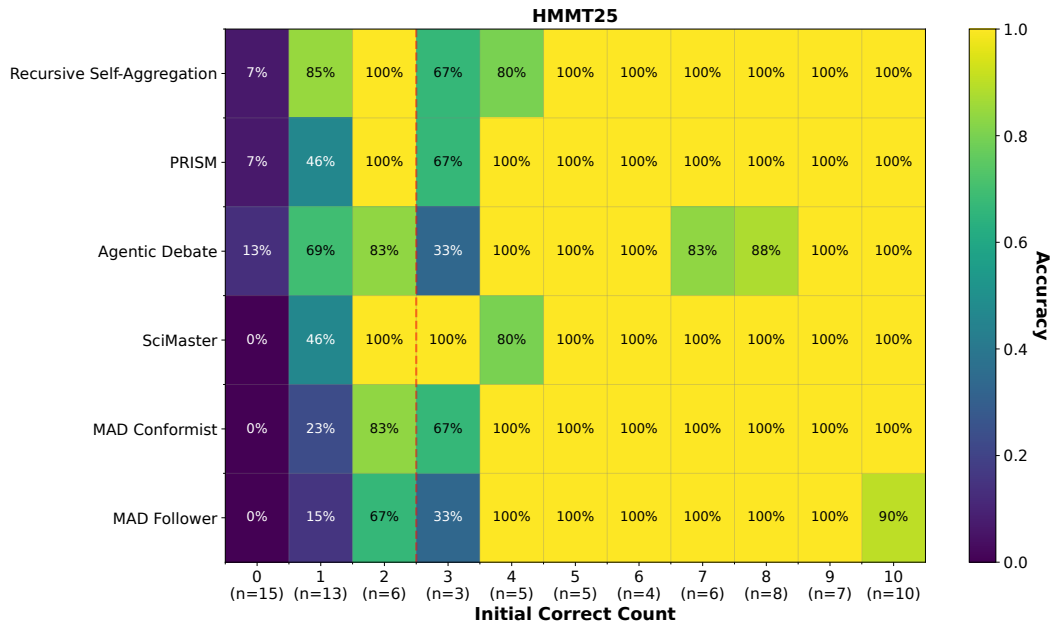


Figure 14: **HMMT25 performance conditioned on initial population quality.** Each column groups problems by how many correct solutions appear in the initial candidate pool, and each cell reports the final accuracy after refinement and majority voting. While most methods struggle when few correct candidates are present at the start, PRISM maintains substantially higher accuracy in these low-correctness regimes, which shows stronger resilience to weak initial populations.

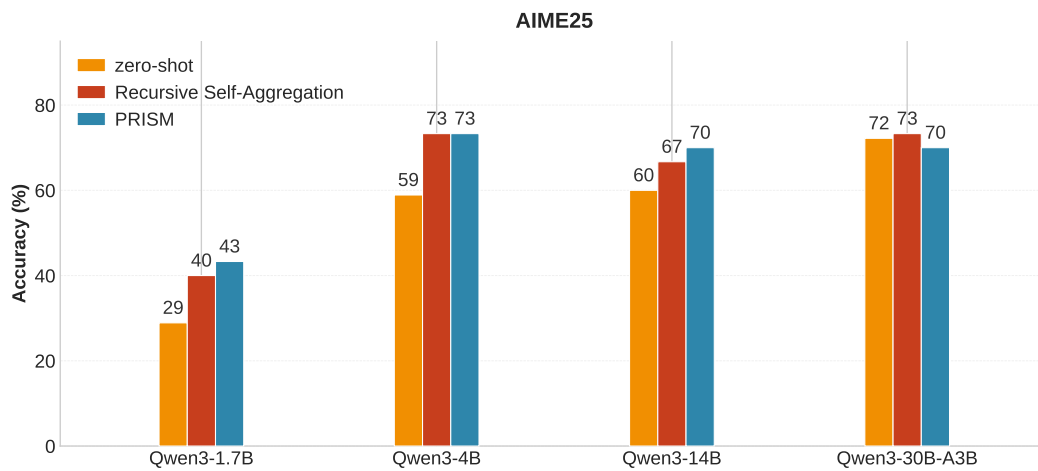


Figure 15: **AIME25** results on **Qwen3** across model sizes. The bar chart compares zero-shot, Recursive Self-Aggregation, and PRISM across Qwen3-1.7B, 4B, 14B, and 30B-A3B. PRISM consistently improves over zero-shot performance across model sizes, with the largest gains observed for smaller models.

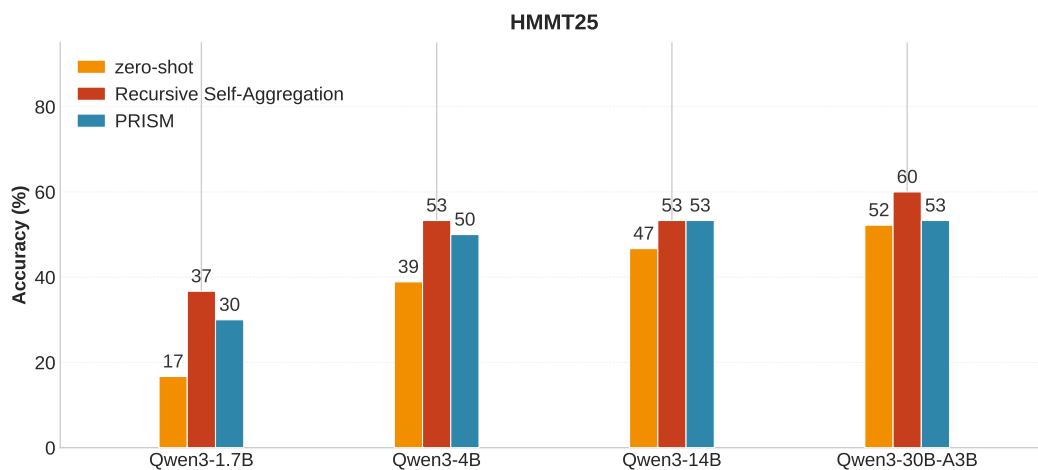


Figure 16: **HMMT25** results on **Qwen3** across model sizes. The bar chart compares zero-shot, Recursive Self-Aggregation, and PRISM across Qwen3-1.7B, 4B, 14B, and 30B-A3B. PRISM consistently improves over zero-shot performance across model sizes, with the largest gains observed for smaller models.

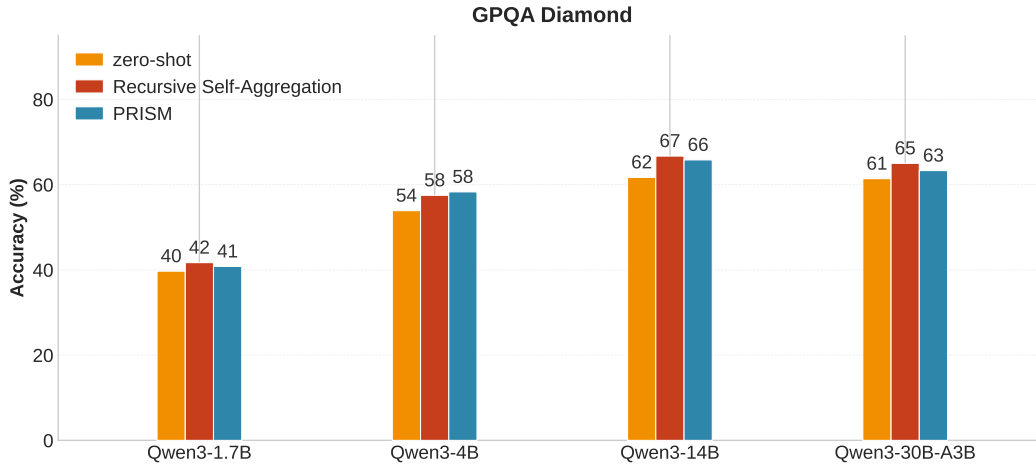


Figure 17: **GPQA Diamond results on Qwen3 across model sizes.** The bar chart compares zero-shot, Recursive Self-Aggregation, and PRISM across Qwen3-1.7B, 4B, 14B, and 30B-A3B. PRISM consistently improves over zero-shot performance across model sizes, with the largest gains observed for smaller models.

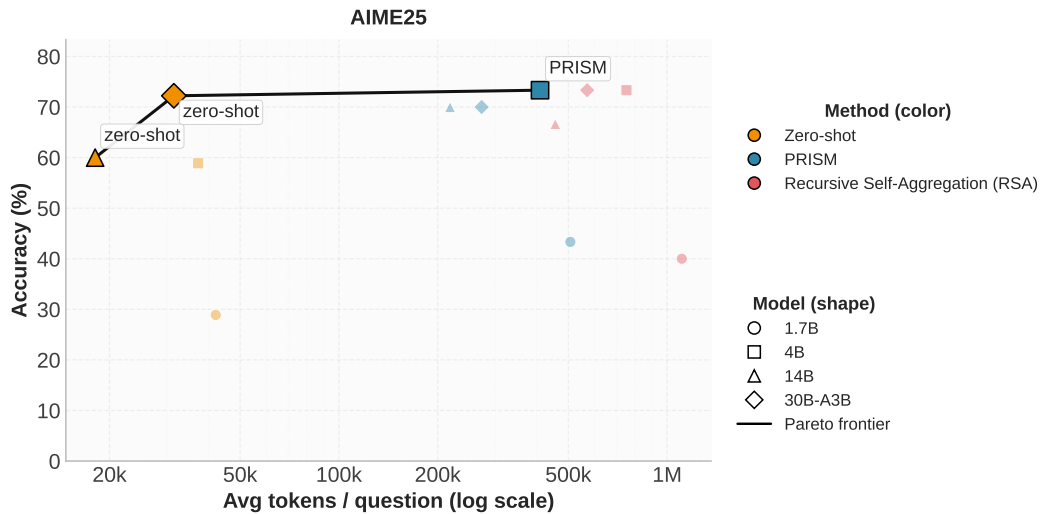


Figure 18: **AIME25 compute-accuracy tradeoff on Qwen3.** Each point corresponds to a method (color) and model size (marker shape), with the x-axis showing average tokens per question (log scale) and the y-axis showing accuracy. The Pareto frontier highlights that PRISM remains competitive under fixed compute budgets, which indicates that its gains are not driven solely by increased token usage.

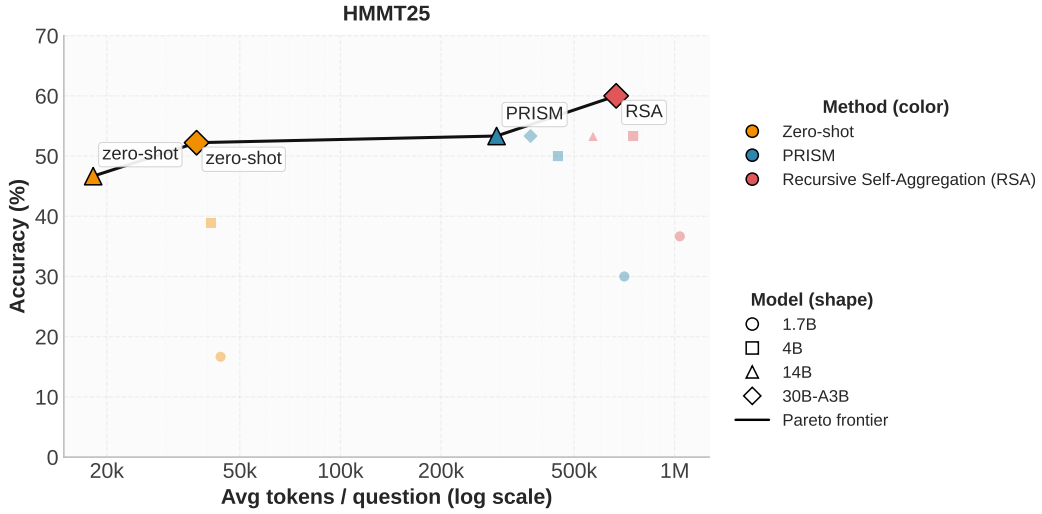


Figure 19: **HMMT25 compute-accuracy tradeoff on Qwen3**. Each point corresponds to a method (color) and model size (marker shape), with the x-axis showing average tokens per question (log scale) and the y-axis showing accuracy. The Pareto frontier highlights that PRISM remains competitive under fixed compute budgets, which indicates that its gains are not driven solely by increased token usage.

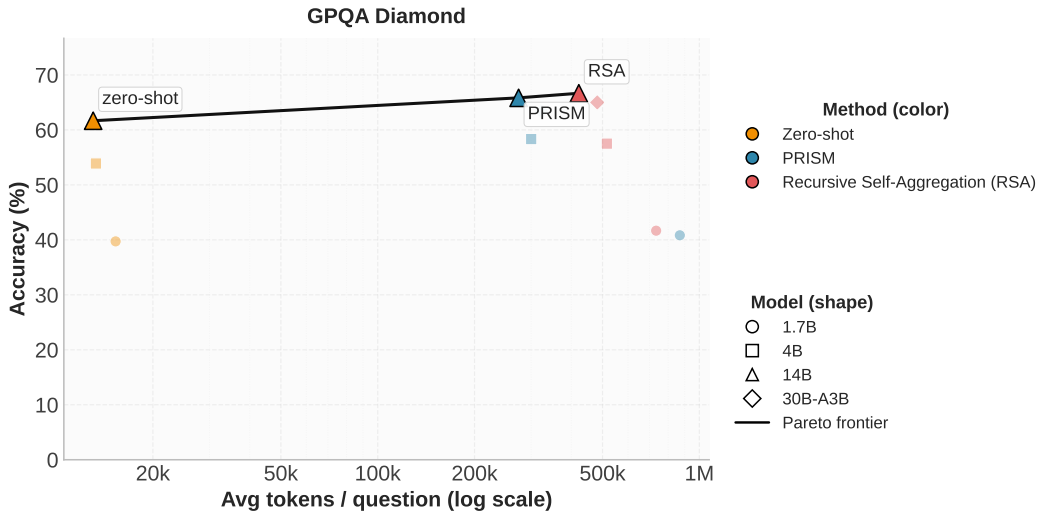


Figure 20: **GPQA Diamond compute-accuracy tradeoff on Qwen3**. Each point corresponds to a method (color) and model size (marker shape), with the x-axis showing average tokens per question (log scale) and the y-axis showing accuracy. The Pareto frontier highlights that PRISM remains competitive under fixed compute budgets, which indicates that its gains are not driven solely by increased token usage.

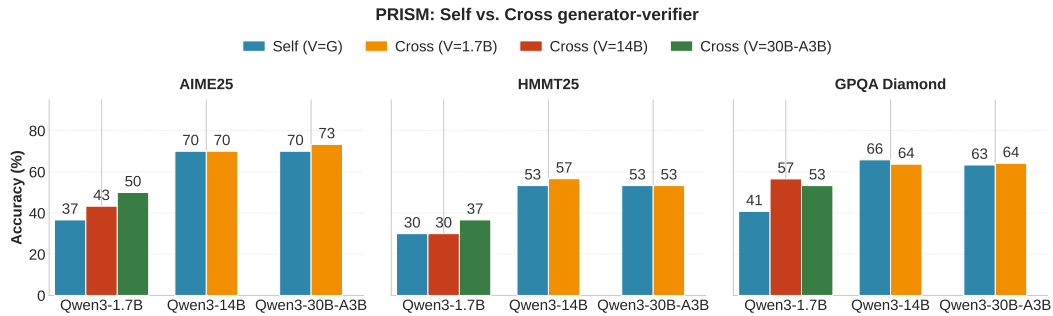


Figure 21: **Cross generator-verifier scaling on Qwen3.** Bars report PRISM accuracy when the generator is fixed and the verifier varies, comparing self-verification (V=G) with cross-verification using different verifier sizes. Performance improves as verifier strength increases, with the largest gains occurring when the verifier is larger than the generator.

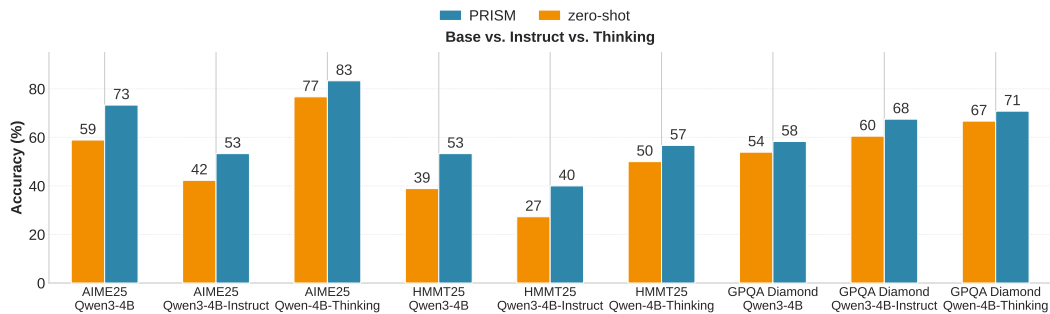


Figure 22: **Model-type comparison on Qwen3-4B: Base vs. Instruct vs. Thinking variants.** Bars compare zero-shot and PRISM across closely related variants for each dataset. PRISM consistently improves performance, with larger gains on weaker variants, thereby narrowing the gap to stronger tuned models.